Optical MIMO-TDS-OFDM with Generalized LED Index Modulation

AZZA ALAMIR and HAMADA ESMAIEL
Electrical Engineering Department, Faculty of Engineering, Aswan University, 81542, Egypt
azzaalamer@yahoo.com, h.esmaiel@aswu.edu.eg.

Abstract: - Recently, generalized light emitting diode (LED) index modulation scheme orthogonal frequency division multiplexing (GLIM-OFDM) was suggested to Li-Fi technology. In this paper, we proposed time domain synchronous OFDM (TDS-OFDM) as a modulation technique for generalized LED. In this scheme, TDS operates over the visible light communication channel to mitigate the inter-symbol interference by separating the complex TDS-OFDM signals into real and imaginary parts, then, exploiting the spatial multiplexing principle to transmit these signals through the channel. The suggested scheme performances based on computer simulation are explained in terms of BER performance and energy efficiency.

Key-Words: - Generalized LED index modulation (GLIM), Time domain synchronous (TDS), OFDM, VLC.

1 Introduction

Due to the increasing demand for high-speed data transport and mobility, wireless communication is very important technology in our lives. The low bandwidth problem restricts the wireless communication and visible light communication (VLC) try to solve this problem by providing a huge bandwidth [1]. The VLC uses visible light's wavelength interval, ranges between 380 nm and 780 nm corresponding to a frequency spectrum of 430 THz to 790 THz. Li-Fi, as introduced by its inventor, Harald Haas, is a multiple access version of the legacy VLC for realizing fully wireless networks including point-to-multi point and multi point-to-point communication, resource management, interference management, etc. [2]. Although Li-Fi manifests itself as a strong candidate for multiple Gbps transmissions over using mmWave band due to its wide deployment, low cost, high energy efficiency, ultra-small cell size (atto-cell), high security, etc., it comes with many technical challenges put it far from playing solely.

As the date rate increases, multi-path channel characteristics are becoming more dominant, resulting in the inter-symbol interference (ISI). In conventional OFDM the cyclic prefix (CP) is used as guard interval between adjoining OFDM symbols to avoid the inter-symbol interference (ISI) as well as the inter-carrier interference (ICI). However, the CP consists of unknown data, so some dedicated frequency-domain pilots are required for channel estimation and synchronization, thus the total system spectral efficiency is reduced. Its major difference lies in time-domain synchronous OFDM (TDS-OFDM) inserts pseudorandom noise (PN) sequence as a guard interval between the OFDM data symbols. This is the key technology applied in the Chinese digital television network [3]. The PN training sequence is known at the receiver and can be used for synchronization and channel estimation. Therefore, training pilots in frequency-domain used in CP-OFDM and ZP-OFDM could be saved in order to improve the spectral efficiency [4-6].

For high-speed data transmission, single carrier modulation techniques (SCM) suffers from ISI caused by frequency selective VLC channels and need complex channel equalizers. On the other hand, multicarrier modulation techniques (MCM) such as OFDM is used to eliminate ISI caused by a dispersive channel. OFDM has advantage of requiring single tap equalizer at the receiver. The MCM has efficient bandwidth but with low efficiency. Unfortunately, the OFDM MCM generated signals are complex and bipolar in nature, the bipolar signals cannot be transmitted in an intensity modulated/direct detection (IM/DD) optical wireless system, due to the intensity of light cannot be negative. OFDM signals designed for IM/DD systems must be real and non-negative. This can be achieved by imposing Hermitian symmetry on the rest of OFDM frame to enforce the OFDM time domain signal output into the real domain [7].

There are several different techniques of OFDM for IM/DD systems to ensure signal be real and positive such as DC-biased optical OFDM (DCO-OFDM) using direct current bias. This method brings an increase in total electrical power consumption, but without further loss in spectral efficiency. The asymmetrically clipped optical OFDM (ACO-OFDM), which inserts zeros on negative values and only the positive parts transmit data symbols. Although there is negligible DC-bias, the scheme sacrifices 50% spectral efficiency compared to DCO-OFDM for the same quadrature amplitude modulation (QAM) constellation size [8].

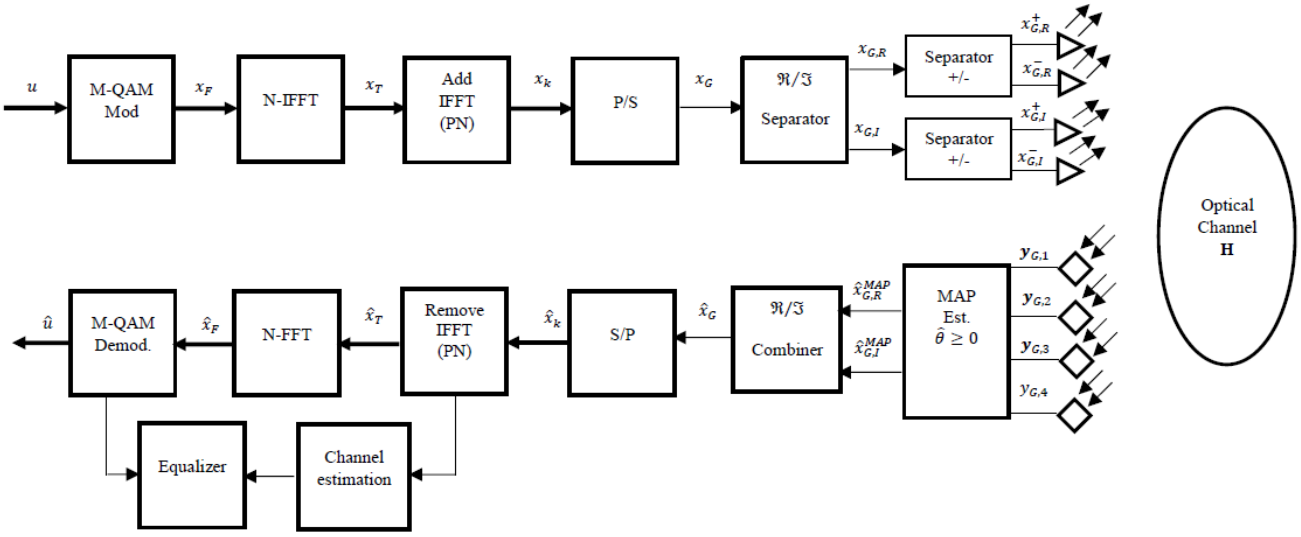

Figure 1, Block diagram of the proposed GLIM-TDS-OFDM scheme for a 4× 4 MIMO-VLC system.

In this work, we propose a new optical OFDM scheme for MIMO-VLC systems, called GLIM-TDS-OFDM which does not demand Hermitian symmetry and DC bias to operate over frequency-selective MIMO optical channels to cope with VLC channels effects. In the proposed scheme, Separator is used to separate the complex time-domain OFDM signals into their real and imaginary parts, and then these signals are transmitted over the MIMO-VLC channel by using spatial multiplexing principle. Higher spectral and power efficiencies can be achieved by encoding the sign information of the complex signals to the location of transmitting LEDs. Moreover, a novel conditional maximum a posteriori probability (MAP) estimator is employed to estimate those real and imaginary parts of the OFDM signals at the receiver [9].

The rest of the paper is organized as follows. In Section 2, the system model for GLIM-TDS-OFDM is analyzed. The design of its receiver based on the conditional MAP estimator has been introduced in Section 3. Channel estimation based on SOMP is proposed in section 4. Simulation results are provided in Section 5. Some concluding remarks are made in Section 6.

Notation: Bold lower (capital) case letters indicate vectors (matrices). Real normal distributions are given by $\mathcal{N}(\mu, \sigma_w^2)$ where μ and σ_w^2 represent the mean and the variance respectively, as well as complex normal distributions, are given by (μ, σ_w^2). $\mathbb{R}$ denotes the ring of real numbers.

2 System Model of GLIM-TDS-OFDM

Figure 1, shows the system model of the GLIM-TDS-OFDM transmitter. The information bit vector u, which contain $N \log_2(M)$ information bit, where N is the number of OFDM sub-carriers and M is considered signal constellation size like (M-QAM). In the proposed scheme, the OFDM modulator directly processes the complex frequency-domain OFDM frame x_F. The TDS-OFDM symbol $x_k = [x_{k,0}, x_{k,1}, \cdots, x_{k,N-1}]^T$ comprises known training sequence $c_i = [c_{i,0}, c_{i,1} \cdots c_{i,M-1}]^T$ and OFDM data block $d_T = [x_{t,0}, x_{t,1}, \cdots x_{t,N-M-1}]^T$.

$$x_k = \begin{bmatrix} c_i \\ d_T \end{bmatrix}_{N\times 1}. \quad (1)$$

The OFDM symbol vector are bipolar elements and complex-valued, so it cannot be transmitted directly over a VLC channel. In order to overcome this problem, the real and imaginary parts of the complex signal x_G are separated by the real-imaginary separator after parallel-to-serial (P/S) conversion as, $x_G = x_{G,R} + jx_{G,I}$. Afterwards, the resulting real, but bipolar signals $x_{G,R}$ and $x_{G,I}$ are applied to the positive-negative $(+/-)$ separators to acquire the following positive-valued signals:

$$x^+_{G,R} = \begin{cases} x_{G,R} & \text{if } x_{G,R} > 0 \\ 0 & \text{if } x_{G,R} < 0 \end{cases}, \quad x^-_{G,R} = \begin{cases} 0 & \text{if } x_{G,R} > 0 \\ -x_{G,R} & \text{if } x_{G,R} < 0 \end{cases} \quad (2)$$

$$x_{G,I}^{+}=\begin{cases}x_{G,I} & \text{if } x_{G,I}>0\\ 0 & \text{if } x_{G,I}<0\end{cases},\ x_{G,I}^{-}=\begin{cases}0 & \text{if } x_{G,I}>0\\ -x_{G,I} & \text{if } x_{G,I}<0\end{cases} \quad (3)$$

The positive and real OFDM time samples $x_{G,R}^{+}$, $x_{G,R}^{-}$, $x_{G,I}^{+}$ and $x_{G,I}^{-}$ are transmitted over the $n_R \times 4$ optical MIMO channel (represented by **H**) for $k = 0,1 \cdots, N-1$ as in [9] :

$$y = \boldsymbol{H}\boldsymbol{x} + \boldsymbol{n}, \quad (4)$$

where the received vector $y = \left[y_{k,1} \cdots y_{k,n_R}\right]^T$ is contained electrical signals obtained from photo detector at the receiver. $\boldsymbol{n} \in \mathbb{R}^{n_R \times 1}$ indicates a vector of additive white Gaussian noise, that models the shot noise and thermal noise due to ambient light. The $\boldsymbol{n}$ elements follow $\mathcal{N}(0, \sigma_w^2)$ distribution, where $\mathcal{N}(\mu, \sigma_w^2)$ is added to the received signals in the electrical domain. The transmitted signal vector $x \in \mathbb{R}^{4\times 1}$ can be formed for GLIM-TDS-OFDM as:

$$x_G = \left[\, x_{G,R}^{+} \;\; x_{G,R}^{-} \;\; x_{G,I}^{+} \;\; x_{G,I}^{-}\right]^{\mathrm{T}}. \quad (5)$$

The $4 * 4$ optical MIMO channel is represented by:

$$H = \begin{bmatrix} h_{1,1} & h_{1,2} & h_{1,3} & h_{1,4} \\ h_{2,1} & h_{2,2} & h_{2,3} & h_{2,4} \\ h_{3,1} & h_{3,2} & h_{3,3} & h_{3,4} \\ h_{4,1} & h_{4,2} & h_{4,3} & h_{4,4} \end{bmatrix}, \quad (6)$$

where $h_{r,t}$ denotes a directed line-of-sight dc channel gain link between the receiver *r* located at distance d and angle ϕ with respect to the transmitter *t*. this line-of-sight dc channel gain can be approximated as [10]:

$$h_{r,t} = \begin{cases} \frac{A_r(m_1+1)}{2\pi d^2} cos^{m_1}(\phi) T_s(\psi) g(\psi)\, cos(\psi) & 0 \le \psi \le \Psi_c \\ 0 \qquad elsewhere \end{cases} \quad (7)$$

where $T_s(\psi)$ is an optical band-pass transmitted signal, $g(\psi)$ is the concentrator optical gain, ψ is the incidence angle with respect to the receiver axis and the field of view (FOV) semi-angle at the receiver modeled by Ψ_c. The Lambertian emission order is $m_1 = -\ln 2 / ln\left(cos\, \Phi_{1/2}\right)$ and $\Phi_{1/2}$ is the semi-angle of a transmitter. In this study, we consider the average electrical signal-to-noise ratio (SNR) at the receiver as given in [9]:

$$SNR = \frac{P_{RX}^{elec}}{\sigma_n^2} = \frac{1}{\sigma_n^2}\zeta\left(P_{RX}^{opt}\right)^2, \quad (8)$$

Where P_{RX}^{elec} is the average electrical power at the receiver and ζ denotes the electrical-to-optical conversion factor that is taken in this paper as unity. Then, the average received optical power can be expressed as:

$$P_{RX}^{opt} = \frac{1}{n_R}\sum_{r=1}^{n_R}\sum_{t=1}^{n_T} h_{r,t} I, \quad (9)$$

Where I is the optical intensity mean being emitted, suppose this means is $E\{x_F^H\, x_F\} = N$. In the proposed GLIM-TDS-OFDM-QAM constellation normalized to have unit-energy symbols. If its inverse fast Fourier transform operation satisfies the normalization of $E\{x_T^H\, x_T\} = N$, the x_T elements follow $\mathcal{CN}(0,1)$ distribution for large N values. Considering that $x_{G,I}$ and $x_{G,R} \sim \mathcal{N}(0, 1/2)$, due to the symmetry, all two elements of x_G have clipped Gaussian distribution having the following probability density function:

$$p_{x_{G,R(I)}}(v) = \left(1/\sqrt{\pi}\right) exp(-v^2)u(v) + \frac{1}{2}\delta(v), \quad (10)$$

where $\delta(v)$ and $u(v)$ denote Dirac delta functions and unit step, respectively. Then, the average optical power emitted from the LED of the GLIM-TDS-OFDM scheme can be obtained as:

$$I = E\{x_{G,R(I)}\} = \int_0^\infty v\, p_{x_{G,R(I)}}(v) dv = 1/\left(2\sqrt{\pi}\right). \quad (11)$$

3 Conditional Estimator of GLIM-TDS-OFDM

The transmission model given in (4) differs from the classical single-carrier systems due to the real-valued of received vector. Also, the transmitted column vector x has been clipped due to the AWGN vector distribution. Hence, we must first construct the complex valued signals to obtain the estimated frequency domain by the OFDM block x_k and then the received signal vector y forward to the OFDM QAM demodulator. The zero-forcing (ZF) equalizer is used to restore the transmitted signal x symbols as follows:

$$\hat{\mathrm{x}}^{\mathrm{ZF}} = \mathbf{H}^{-1}\mathrm{y}. \quad (12)$$

After ZF estimator operation, receiver can determine the indices of the active LEDs and corresponding signals by choosing the higher magnitude signals from $\hat{x}^{ZF}$[11]. In spite of its simplicity, the ZF estimator can significantly boost the noise power through multiplication of noise with reciprocal of the channel. Moreover, it does not consider the probability distribution of **x** as a priori information, it may produce negative-valued estimates. We propose a MAP estimator for the GLIM-TDS-OFDM scheme to overcome the aforementioned drawbacks of the ZF estimator due to containing all the knowledge about the signal vector **x** . By defining the column vectors of $\boldsymbol{H}$ as $\boldsymbol{H} = [h_1\ h_2\ h_3\ h_4]$ and observe signals given in (4), it can be reformulated as:

$$y = h_m \bar{x}_{G,R} + h_n \bar{x}_{G,I} + n, \quad (13)$$

where $\bar{x}_{G,R} = |x_{G,R}|$, $\bar{x}_{G,I} = |x_{G,I}|, m \in \{1,2\}$ and $n \in \{3,4\}$. It can be easily shown that $\bar{x}_{G,R}$ and $\bar{x}_{G,I}$ have half-normal a folded Gaussian distribution as:

$$p_{\bar{x}_{G,R(I)}}(v) = \frac{1}{\sqrt{\pi}} e^{-v^2} u(v). \quad (14)$$

As a result, for a given pair (m, n), the conditional MAP estimator of $\bar{x}_{G,R}$ and $\bar{x}_{G,I}$ can be expressed as:

$$\left(\tilde{x}_{G,R}^{(m,n)}, \tilde{x}_{G,I}^{(m,n)}\right) = \arg \max_{\bar{x}_{G,R}, \bar{x}_{G,I}} p\left(\bar{x}_{G,R}, \bar{x}_{G,I}/y\right), \quad (15)$$

$$\left(\tilde{x}_{G,R}^{(m,n)}, \tilde{x}_{G,I}^{(m,n)}\right) = \arg \max_{\bar{x}_{G,R}, \bar{x}_{G,I}} p(\bar{x}_{G,R}, \bar{x}_{G,I}/y) p(\bar{x}_{G,R}) p(\bar{x}_{G,I}). \quad (16)$$

where $p\left(\bar{x}_{G,R}, \bar{x}_{G,I}/y\right)$ is the probability density function of $\bar{x}_{G,R}$ and $\bar{x}_{G,I}$ conditioned on received signal y. Since the conditional distribution of received signal y is $\mathcal{N}\left(h_m \bar{x}_{G,R} + h_n \bar{x}_{G,I}, \sigma_w^2\right)$, by deleting the constants from (16), the conditional MAP estimator of $\bar{x}_{G,R}$ and $\bar{x}_{G,I}$ can be defined as:

$$\left(\tilde{x}_{G,R}^{(m,n)}, \tilde{x}_{G,I}^{(m,n)}\right) = \arg \max_{\bar{x}_{G,R}, \bar{x}_{G,I}} exp\left(-\left[\bar{x}_{G,R}^2 + \bar{x}_{G,I}^2\right]\right) \times exp\left(-\left\|y - h_m \bar{x}_{G,R} - h_n \bar{x}_{G,I}\right\|^2 / (2\sigma_w^2)\right). \quad (17)$$

Taking the logarithm and made simple manipulations of (17), the MAP estimator of $\bar{x}_{G,R}$ and $\bar{x}_{G,I}$ follows that:

$$\left(\tilde{x}_{G,R}^{(m,n)}, \tilde{x}_{G,I}^{(m,n)}\right) = \arg \max_{\bar{x}_{G,R}, \bar{x}_{G,I}} M^{MAP}\left(m, n, \bar{x}_{G,R}, \bar{x}_{G,I}\right), \quad (18)$$

where $M^{MAP}\left(m, n, \bar{x}_{G,R}, \bar{x}_{G,I}\right)$ is the MAP estimation metric expressed as:

$$M^{MAP}\left(m, n, \bar{x}_{G,R}, \bar{x}_{G,I}\right) = \left\|y - h_m \bar{x}_{G,R} - h_n \bar{x}_{G,I}\right\|^2 + 2\sigma_w^2\left(\bar{x}_{G,R}^2 + \bar{x}_{G,I}^2\right). \quad (19)$$

(19) using $\|e\| = e^{\mathrm{T}} e$ and after some algebra, can be simplified as:

$$M^{MAP}\left(m, n, \bar{x}_{G,R}, \bar{x}_{G,I}\right) = A\bar{x}_{G,R}^2 + B\bar{x}_{G,I}^2 + C\bar{x}_{G,R} + D\bar{x}_{G,I} + E\bar{x}_{G,R}\bar{x}_{G,I}, \quad (20)$$

where $A = h_m^T h_m + 2\sigma_w^2$, $B = h_n^T h_n + 2\sigma_w^2$, $C = -2y^T h_m$, $D = -2y^T h_n$ and $E = 2h_m^T h_n$.

$$\tilde{x}_{G,R}^{(m,n)} = \left[\frac{2BC - ED}{E^2 - 4AB}\right]^+ \quad \tilde{x}_{G,I}^{(m,n)} = \left[\frac{2AD - EC}{E^2 - 4AB}\right]^+, \quad (21)$$

where $\boldsymbol{q} = \left[\bar{x}_{G,R} \ \bar{x}_{G,I}\right]^T$, the minimization of (20) is equivalent to a well-known constraint quadratic programming problem defined as [12]:

$$\min_{\boldsymbol{q}} \left\{\frac{1}{2}\boldsymbol{q}^T \boldsymbol{Q}\boldsymbol{q} + \boldsymbol{b}^T \boldsymbol{q}\right\} \quad \text{subject to } \boldsymbol{A}\boldsymbol{q} \leq \boldsymbol{c}. \quad (22)$$

Please note that, the optimal estimates of $\boldsymbol{q}$ in (21) as well guarantees that $\tilde{x}_{G,R}^{(m,n)} \geq 0$ and $\tilde{x}_{G,I}^{(m,n)} \geq 0$ for all **Q** and **b** and regardless of the received SNR and channel conditions.

Algorithm 1: Conditional MAP Estimator

1: **for** m=1:2 **do**
2: **for** n=3:4 **do**
3: Estimate, $\tilde{\boldsymbol{x}}_{\boldsymbol{G,R}}^{(\boldsymbol{m,n})}$ and $\tilde{\boldsymbol{x}}_{\boldsymbol{G,I}}^{(\boldsymbol{m,n})}$ values from (**21**)
4: Estimate, $(\hat{\boldsymbol{m}}, \hat{\boldsymbol{n}})$ indices from (**22**)
5: **end for**
6: **end for**

To determine the indices of the active LEDs, we estimate m and n as well as in (18), the condition MAP estimator obtains $\tilde{x}_{G,R}^{(m,n)}$ and $\tilde{x}_{G,I}^{(m,n)}$ for all possible (m, n) pairs, and then gets the unconditional (actual) estimates of $\bar{x}_{G,R}$ and $\bar{x}_{G,I}$ as follows:

$$(\hat{m}, \hat{n}) = \arg \max_{m,n} M^{MAP}\left(m, n, \tilde{x}_{G,R}^{(m,n)}, \tilde{x}_{G,I}^{(m,n)}\right),$$
$$\hat{x}_{G,R}^{MAP} = \tilde{x}_{G,R}^{(\hat{m},\hat{n})}, \quad \hat{x}_{G,I}^{MAP} = \tilde{x}_{G,I}^{(\hat{m},\hat{n})}. \quad (23)$$

The conditional MAP estimator steps can be summarized as shown in Algorithm 1. The complex OFDM signal $\hat{x}_G$ can be calculated by the $\Re/\Im$ combiner as:

$$\hat{x}_{G,R} = \begin{cases} \hat{x}_{G,R}^{MAP} & if\ m = 1 \\ -\hat{x}_{G,R}^{MAP} & if\ m = 2 \end{cases}, \hat{x}_{G,I} = \begin{cases} \hat{x}_{G,I}^{MAP} & if\ m = 3 \\ -\hat{x}_{G,I}^{MAP} & if\ m = 4 \end{cases}, \quad (24)$$

$$\hat{x}_G = \pm\tilde{x}_{G,R}^{(\hat{m},\hat{n})} \pm j\tilde{x}_{G,I}^{(\hat{m},\hat{n})}, \quad (25)$$

Finally, these will be applied to serial to parallel (S/P) conversion.

4 Channel Estimation Using SOMP Technique

The GLIM-MIMO-TDS-OFDM channel can be estimated based on SOMP algorithm. Where, the received PN sequence over VLC multipath channel y_i can be denoted as:

$$y_i = \Phi_i h_i + n_i. \quad (26)$$

where,

$$\Phi_i = \begin{bmatrix} c_{i,L_{ch}-1} & c_{i,L_{ch}-2} & \cdots & c_{i,0} \\ c_{i,L_{ch}} & c_{i,L_{ch}-1} & \cdots & c_{i,1} \\ \vdots & \vdots & \vdots & \vdots \\ c_{i,M-1} & c_{i,M-2} & \cdots & c_{i,M-L_{ch}} \end{bmatrix}, \quad (27)$$

where L_{ch} is the maximum channel tap delay. The VLC channel impulse response can be estimated based on SOMP by solving the following nonlinear optimization problem as in [13]:

$$\widehat{\boldsymbol{H}} = arg \min_{H \in C^{L \times R}} \|Y - \Phi \boldsymbol{H}\|_{p,q}. \quad (28)$$

Then, classical OFDM procedures can be applied to FFT and *M*-ary demodulation to get the estimate $\hat{\boldsymbol{u}}$ of the information bit vector.

5 Simulation Results

In this section, we investigate the communication system performance by testing coded and uncoded BER performance of GLIM-MIMO-OFDM. In all simulation,

the number of sub-carrier is T=1024 with QPSK modulation technique. For the coded case, random information bits are first encoded by rate 1/2 of the convolutional encoder with generate polynomial and interleaved by a block interleaver of depth 8 before to QPSK modulation. For uncoded case, the information bits are generated and modulated by QPSK modulation. In all simulation results, the simulated channel is averaged over 500 runs. The VLC channel is used as in [14].

5.1 Subcarrier Usage Index Utilization

In this paper, the effect of using proposed GLIM-TDS-OFDM in subcarrier usage index (the percentage of the sub-carrier number used for useful information data to the total number of subcarrier) is evaluated. The normalized subcarrier usage index utilization, γ_o, of the different OFDM schemes, can be calculated as:

$$\gamma_o = \frac{T_{data} - T_{pilot}}{T_{data} + M}. \quad (29)$$

where numbers of data subcarriers are represented by T_{data}, numbers of pilot subcarriers are represented by T_{pilot}, and M is the guard interval length. Figure 2, shows the subcarrier usage index of the TDS-OFDM compared to CP-OFDM as a function of the guard interval length. As shown in Figure 2, the TDS-OFDM outperform the conventional (CP-OFDM & ZP-OFDM) with more than 5% in subcarrier usage index term when the pilot sequence length is 64.

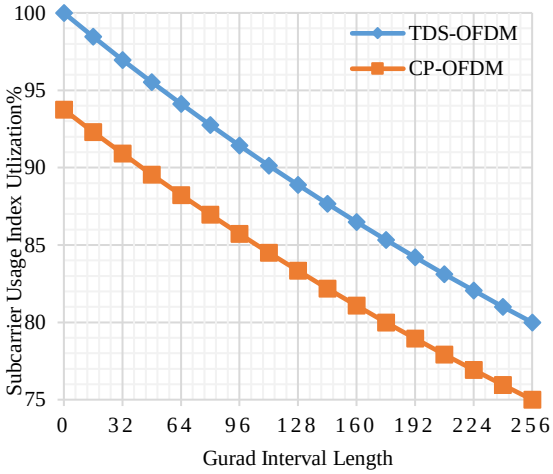

Figure 2: Subcarrier Usage Index Utilization comparison between ZP-OFDM and TDS-OFDM.

5.1 BER Performance of (TDS-OFDM, CP-OFDM and ZP-OFDM) in Li-Fi MIMO System.

In this subsection, we present coded and uncoded BER performance results of the GLIM-OFDM system of TDS, CP, and ZP. In Figure 3, based on perfect channel estimation, the BER performance curves the ZP-OFDM is the goodies BER comparing to the TDS-OFDM and CP-OFDM due to the remaining inter-block interference between the training sequence and OFDM data blocks. When the channel is estimated based on SOMP in all OFDM sachems for a fair comparison, the TDS-OFDM outperform the conventional OFDM systems where channel estimation based on guard interval length is more efficient than the pilot-based method. Whereas the guard interval length is increased as the channel estimation accuracy increase. Figure 4, shows the BER performance in different OFDM schemes in GLIM-OFDM system operating at the same guard interval values and using the same channel estimation method.

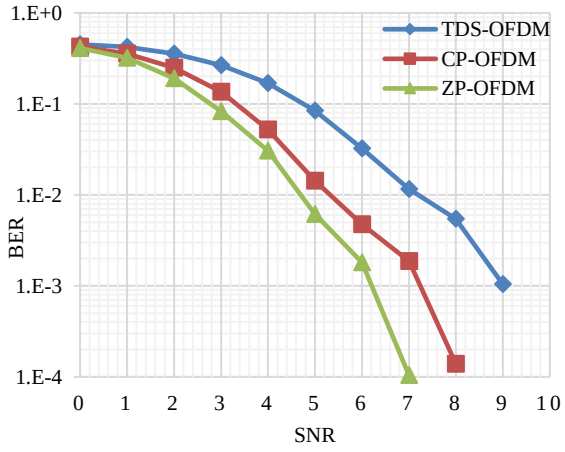

(a)

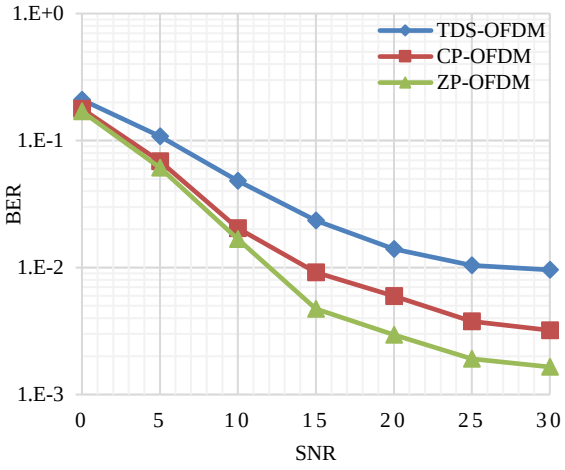

(b)

Figure 3, BER performance comparison in known channel. (a) Coded BER Performance, (b) Uncoded BER Performance.

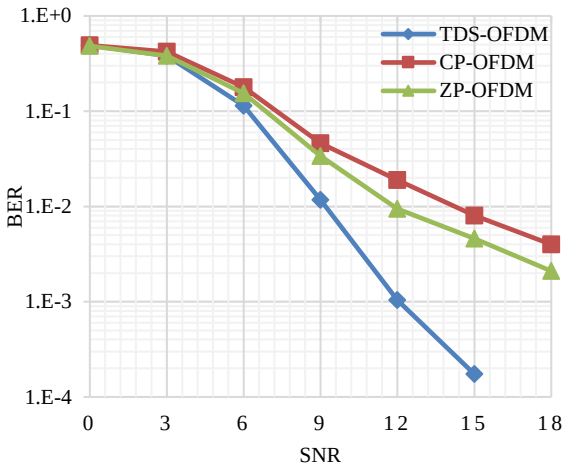

(a)

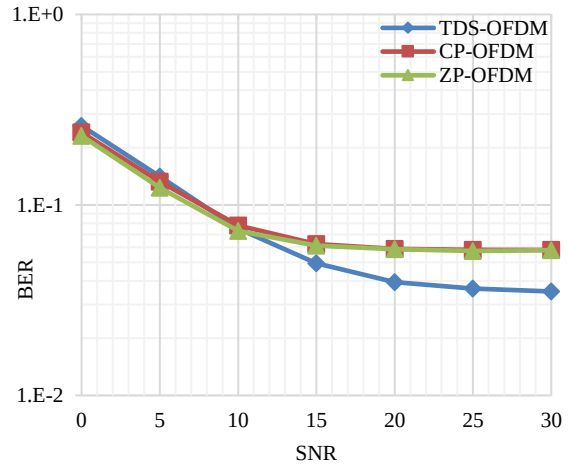

(b)

Figure 4, BER performance comparison in estimation channel. (a) coded BER performance, (b) uncoded BER performance.

6 Conclusion

In this paper, the GLIM-TDS-OFDM scheme has been proposed for frequency selective VLC channel. The scheme uses spatial multiplexing principle and can transmit complex OFDM signals through the optical channel into the real and imaginary part by using separator signal component. This scheme outperforms the conventional OFDM schemes in terms of subcarrier usage index utilization by more than 5%. The subcarrier usage index is a new definition measure the bandwidth efficiently. Also, we conclude from the computer simulations that the proposed GLIM-TDS-OFDM scheme outperforms conventional schemes in terms of BER performance when the channel is estimated due to the accuracy of TDS-OFDM channel estimation methods based on its training sequence.

References:

[1] L. U. Khan, "Visible light communication: Applications, architecture, standardization and research challenges," Digital Communications and Networks, vol. 3, pp. 78-88, 2017.

[2] H. Haas, L. Yin, Y. Wang, and C. Chen, "What is LiFi?," Journal of Lightwave Technology, vol. 34, pp. 1533-1544, 2016.

[3] A. B. Bagade, P. Student, and A. Deshmukh, "Study of Time Domain Synchronous OFDM: Consequences and Solutions."

[4] H. Esmaiel and D. Jiang, "Spectrum and Energy Efficient OFDM Multicarrier Modulation for an Underwater Acoustic Channel," Wireless Personal Communications, vol. 96, pp. 1577-1593, 2017.

[5] H. Esmaiel and D. Jiang, "Zero-pseudorandom noise training OFDM," Electronics Letters, vol. 50, pp. 650-652, 2014.

[6] H. Esmaiel and D. Jiang, "Time reversal time-domain synchronisation orthogonal frequency division multiplexing over multipath fading channels with significant tap delays," Journal of Engineering, pp. 1-10, 2014.

[7] M. S. Islim and H. Haas, "Modulation Techniques for Li-Fi," ZTE Commun, vol. 14, pp. 29-40, 2016.

[8] S. D. Dissanayake and J. Armstrong, "Comparison of aco-ofdm, dco-ofdm and ado-ofdm in im/dd systems," Journal of Lightwave Technology, vol. 31, pp. 1063-1072, 2013.

[9] A. Yesilkaya, E. Basar, F. Miramirkhani, E. Panayirci, M. Uysal, and H. Haas, "Optical MIMO-OFDM with Generalized LED Index Modulation," IEEE Transactions on Communications, 2017.

[10] J. M. Kahn and J. R. Barry, "Wireless infrared communications," Proceedings of the IEEE, vol. 85, pp. 265-298, 1997.

[11] Y. Li, D. Tsonev, and H. Haas, "Non-DC-biased OFDM with optical spatial modulation," in Personal Indoor and Mobile Radio Communications (PIMRC), 2013 IEEE 24th International Symposium on, 2013, pp. 486-490.

[12] S. Boyd and L. Vandenberghe, Convex optimization: Cambridge university press, 2004.

[13] L. Dai, J. Wang, Z. Wang, P. Tsiaflakis, and M. Moonen, "Spectrum-and energy-efficient OFDM based on simultaneous multi-channel reconstruction," IEEE Transactions on Signal Processing, vol. 61, pp. 6047-6059, 2013.

[14] A. Yesilkaya, E. Basar, F. Miramirkhani, E. Panayirci, M. Uysal, and H. Haas, "Optical MIMO-OFDM with generalized LED index modulation," IEEE Transactions on Communications, vol. 65, pp. 3429-3441, 2017.